IOPscience iopscience.iop.org

Home Search Collections Journals About Contact us My IOPscience

Structural phase transitions in germanate analogues of $KTiOPO_4$ investigated by high-resolution neutron powder diffraction

This article has been downloaded from IOPscience. Please scroll down to see the full text article.

1997 J. Phys.: Condens. Matter 9 3833

(http://iopscience.iop.org/0953-8984/9/19/005)

View the table of contents for this issue, or go to the journal homepage for more

Download details:
IP Address: 171.66.16.207
The article was downloaded on 14/05/2010 at 08:39

Please note that terms and conditions apply.

J. Phys.: Condens. Matter **9** (1997) 3833–3851. Printed in the UK PII: S0953-8984(97)81203-9

Structural phase transitions in germanate analogues of $KTiOPO_4$ investigated by high-resolution neutron powder diffraction

E L Belokoneva†, K S Knight‡, W I F David‡ and B V Mill§

† Department of Crystallography, Geological Faculty, Moscow State University, Moscow 199899, Russia

‡ Rutherford Appleton Laboratory, Chilton, Oxon OX11 0QX, UK

§ Physical Faculty, Moscow State University, Moscow 119899, Russia

Received 22 January 1997

Abstract. Structural phase transitions at high temperatures have been investigated in members of a new group of germanate analogues of $KTiOPO_4$ (KTP) with general formula $AMXO_4$, $TlSbOGeO_4$, $RbSbOGeO_4$ and $KTaOGeO_4$, using high-resolution neutron powder diffractometry at the pulsed neutron source ISIS, Rutherford Appleton Laboratory. The temperature-induced ferroelectric–paraelectric phase transition in the KTP structure type, accompanied by a change of space group from $Pna2_1$ to $Pnan$, is continuous second order and is both displacive and order–disorder in nature, in contrast to the purely displacive phase transition in $KTiOPO_4$ produced by high pressure at ambient temperature. The regularity of the increasing values of T_C found in a series of KTP analogues is in agreement with Abrahams–Jamieson–Kurtz (AJK) criteria. The behaviour of the A cations determines the ferroelectric properties; M octahedra together with the A cations make a considerable contribution to the nonlinear optical properties. The redistribution of A cations in the structural holes formed by the framework must be polar, and the cations must not suppress the electronic state of the titanyl bridge oxygens in the chain of octahedra, which is favourable for the existence of a charge transfer excited state delocalized along the TiO_6 chains. The alternating short and long interatomic distances in crystals with good second-harmonic generation (SHG) is typical not only for the M–O bridge, but also for the A–O bridge.

1. Introduction

Potassium titanyl phosphate, $KTiOPO_4$ (KTP), is one of the most effective nonlinear optic materials. The possibility of making a wide range of isomorphic substitutions at the K and Ti positions in the KTP structure gives rise to numerous analogues of KTP amongst the phosphates and arsenates [1].

Recently, an important new isomorphic substitution, that of Si or Ge in the tetrahedrally coordinated position normally occupied by phosphorus, has been explored in the germanates and silicates $AMOXO_4$ in which A is Na, K, Rb, Tl or Ag, M is Sb or Ta and X is Si or Ge. Their crystal structures have been determined at room temperature or below by single-crystal x-ray diffraction [2–14].

According to measurements of the temperature dependence of the second-harmonic generation (SHG) signal $I_{2\omega}$ from powder samples together with dielectric and microcalorimetric data, the ferroelectric phase transitions in these crystals were described

0953-8984/97/193833+19$19.50 © 1997 IOP Publishing Ltd

as second order [6, 15, 16] except that in Tl, Sb germanate, which was reported to be first order [17]. The Curie points T_C of the new ferroelectric compounds determined by different methods are in good agreement and they lie in the temperature range 272–1200 K, which is lower than that for the phosphates and arsenates, so the phase transitions in the silicate and germanate analogues are easier to investigate experimentally.

The study of the high-temperature paraelectric modification and the mechanism of the phase transition is of interest in establishing the relationship between structure and the ferroelectric and nonlinear optic properties of KTP-like compounds.

Before the discovery of the new group of KTP analogues, the structure of the paraelectric phase of $TlSbOPO_4$ was determined from single-crystal neutron diffraction data collected at 923 K [18]. This compound was chosen since it exhibited the lowest T_C but the final agreement factors were high, $R = 0.12$ and $R_w = 0.18$. The Tl thermal ellipsoid was very elongated in the c-direction, but attempts to model this feature by splitting the Tl site were inconclusive. The transition was assumed to be displacive and second order in character.

Single-crystal X-ray diffraction data obtained at different temperatures have been used to determine the structures of both modifications of the new KTP analogue $TlSbOGeO_4$ [10] and, more recently, those of the K and Rb germanates and the Na and K silicates, all four compounds having Sb in the M site [19]. Annealing and quenching $AgSbOSiO_4$ from temperatures in the range 800–300 °C gave the paraelectric modification, which was refined also by single-crystal x-ray diffraction [13, 14].

The phase transition in $KTiOPO_4$, $T_C = 1207$ K, has been studied by Kaduk and collaborators using high-resolution neutron powder diffraction and the results were presented during an ACA meeting [20].

We now report results obtained from high-resolution neutron powder diffractometry using HRPD at the pulsed neutron source ISIS, Rutherford Appleton Laboratory, on the structural phase transition in members of the new group of germanates: $TlSbOGeO_4$, $RbSbOGeO_4$ and $KTaOGeO_4$, which have $T_C = 272$, 450 and 700 K, respectively. The structures of the HT modifications have been refined and the ferroelectric–paraelectric phase transition examined in detail. Precise values of the lattice parameters and unit cell volume as a function of temperature have allowed us to determine T_C from the diffraction data. These data have also enabled us to isolate the structural parameters responsible for the phase transition and to investigate its order and mechanism.

2. Experimental details

TlSb, RbSb and KTa germanates were first obtained by solid-phase synthesis at high temperatures and their single-crystals were then grown from non-stoichiometrical melts of A_2O–M_2O_5–XO_2 systems. The powder specimens of the three compounds for the diffraction measurements were prepared from single-crystal material by grinding–sieving so that the particle size was less than 150 μm. Cylindrical vanadium cans with diameter 11 mm and height 76 mm were filled with powders having approximate volumes of 3000 mm^3 for Tl, Sb and Rb, Sb and 1600 mm^3 for K, Ta germanates.

Using a cryostat or furnace as appropriate, diffraction data were collected in the backward-angle detector banks in the temperature interval from 260 to 300 K for $TlSbOGeO_4$, from 433 to 503 K for $RbSbOGeO_4$ and from 690 to 753 K for $KTaOGeO_4$. Time of flight data between 30 and 130 ms were recorded, corresponding to a range of d-spacings of 0.6–2.6 Å (exact ranges for each spectrum are given in table 1). Structural analysis was performed using the Rietveld method and program TF12LS based on the Cambridge Crystallography Subroutine Library (CCSL).

Table 1. Results of the profile refinements. The profile R-factor, $R_p = 100\sum(Y_{diff}/Y_{obs})$. Weighted profile R-factor, $R_w = 100\sqrt{[\sum(\text{weighted difference})^2/\sum(\text{weighted observations})^2]}$.

High-temperature modification of RbSbOGeO$_4$ at 503 K

Time of flight data range, 31.5–122.5 ms 1804 reflections, 37 structural parameters
$R_p = 4.29$, $R_w = 4.51$, $(N - P + C) = 4490$ $\chi^2 = 2.22$ for 4528 observations
$a = 13.412\,46(4)$, $b = 6.726\,71(2)$, $c = 10.726\,11(3)$ AA space group, $Pnan$

Atom	x/a	y/b	z/c	ITF	Occupation
Rb1	−0.1394(5)	0.4505(7)	0.1606(9)	2.17(7)	0.51(1)
Rb2	−0.1380(5)	0.4557(8)	0.0952(8)	2.17(7)	0.49(1)
Sb1	0.1312(3)	1/4	1/4	0.68(6)	
Sb2	0	0	0	0.55(6)	
Ge1	1/4	0.0682(3)	0	0.59(3)	
Ge2	0.0704(2)	3/4	1/4	0.46(4)	
O1	−0.1435(2)	0.0789(3)	0.0180(2)	1.06(4)	
O2	0.0140(2)	0.2001(4)	−0.1288(3)	1.02(5)	
O3	−0.0293(2)	−0.2053(4)	−0.1245(3)	1.00(5)	
O4	−0.1420(2)	0.0440(4)	−0.2888(2)	1.02(5)	
O5	−0.2372(2)	−0.2224(4)	−0.1277(3)	1.55(5)	

High-temperature modification of KTaGeO$_5$ at 753 K

Time of flight data range, 31–121 ms 1925 reflections, 37 structural parameters
$R_p = 3.92$, $R_w = 4.33$, $(N - P + C) = 4490$ $\chi^2 = 2.55$ for 4541 observations
$a = 13.44\,521(5)$, $b = 6.691\,01(2)$, $c = 10.987\,14(4)$ Å space group, $Pnan$

Atom	x/a	y/b	z/c	ITF	Occupation
K1	−0.139(2)	0.442(3)	0.166(2)	5.2(2)	0.42(2)
K2	−0.135(1)	0.464(2)	0.077(2)	5.2(2)	0.58(2)
Ta1	0.1330(3)	0.25	0.25	1.03(6)	
Ta2	0	0	0	1.17(6)	
Ge1	0.25	0.0708(4)	0	1.22(5)	
Ge2	0.0690(2)	0.75	0.25	1.30(5)	
O1	−0.1430(2)	0.0741(4)	0.0192(3)	2.01(6)	
O2	0.0107(2)	0.2081(5)	−0.1252(4)	2.04(6)	
O3	−0.0336(2)	−0.1956(5)	−0.1271(4)	2.01(6)	
O4	−0.1425(3)	0.0411(4)	−0.2859(3)	2.11(6)	
O5	−0.2392(3)	−0.2247(5)	−0.1267(4)	2.28(6)	

The first compound studied was TlSbOGeO$_4$, which has two phase transitions: the lower, ferroelectric–paraelectric at $T_C = 272$ K (which has been reported to be of first rather than second order and therefore an exception to the rest of the group) and an upper phase transition of second order, close by at 286 K. Runs of approximately 1.5 h duration were accumulated at 1 °C intervals through the two transitions (41 data sets) and these data were refined to give accurate cell dimensions. Longer runs for accurate structure refinements were performed at three temperatures: at 260 K in the ferroelectric state below $T_C = 272$ K, but closer to the Curie point than the x-ray diffraction experiment; at 280 K in the intermediate state between 272 and 286 K; and at 423 K in the paraelectric state but at a much higher temperature than the corresponding KTP analogue diffraction experiment. The phase transitions were crossed several times from higher to lower temperature and appeared to be reversible.

For RbSbOGeO$_4$, data were collected for approximately 20 min at 20 °C intervals from 433 to 463 K (16 points) providing patterns which could be refined to give accurate

Table 1. (Continued)

Low-temperature modification of $TlSbOGeO_4$ at 260 K

Time of flight data range, 31.5–22.5 ms 1607 reflections, 75 structural parameters
$R_p = 2.66$, $R_w = 2.97$, $(N - P + C) = 6377$ $\chi^2 = 1.54$ for 6456 observations
$a = 13.360\,34(9)$, $b = 6.667\,87(4)$, $c = 10.765\,1(1)$ Å space group $Pna2_1$

Atom	x/a	y/b	z/c	ITF	Occupation
Tl1	0.3908(8)	0.788(1)	0.665(2)	0.60(5)	0.38(1)
Tl1′	0.3960(6)	0.802(1)	0.599(1)	0.60(5)	0.62(1)
Tl2	0.1103(8)	0.705(2)	0.929(1)	0.60(5)	0.45(2)
Tl2′	0.1148(7)	0.723(1)	0.875(2)	0.60(5)	0.55(2)
Sb1	0.2442(6)	0.248(2)	0.749(1)	0.37(6)	
Sb2	0.3808(2)	0.502(2)	0	0.22(6)	
Ge1	0.4987(6)	0.3170(3)	0.752(1)	0.31(4)	
Ge2	0.1821(2)	0.502(1)	0.501(1)	0.16(4)	
O1	0.4867(4)	0.483(1)	0.873(1)	0.51(5)	
O2	0.9943(6)	0.9630(8)	0.115(1)	0.51(5)	
O3	0.3937(6)	0.164(1)	0.736(1)	0.38(4)	
O4	0.8930(6)	0.674(1)	0.264(1)	0.38(4)	
O5	0.1083(6)	0.296(1)	0.468(1)	0.35(4)	
O6	0.6068(6)	0.791(1)	0.543(1)	0.35(4)	
O7	0.2693(6)	0.550(1)	0.382(3)	0.51(5)	
O8	0.7658(6)	0.045(1)	0.623(1)	0.51(4)	
O9	0.2260(5)	0.957(1)	0.382(1)	0.44(5)	
O10	0.7165(4)	0.4631(1)	0.635(1)	0.44(5)	

$TlSbOGeO_4$ at 280 K

Time of flight data range, 33–20 ms 1544 reflections, 37 structural parameters
$R_p = 2.83$, $R_w = 3.13$, $(N - P + C) = 6402$ $\chi^2 = 1.711$ for 6456 Observations.
$a = 3.360\,25(3)$, $b = 6.667\,98(2)$, $c = 10.764\,71(3)$ Å space group, $Pnan$

Atom	x/a	y/b	z/c	ITF	Occupation
Tl1	−0.1385(3)	0.0325(6)	0.3940(7)	1.1(1)	0.45(1)
Tl2	−0.1425(3)	0.4540(4)	0.1630(6)	0.8(1)	0.55(1)
Sb1	0.1304(2)	1/4	1/4	0.16(5)	
Sb2	0	0	0	0.57(6)	
Ge1	1/4	0.0667(3)	0	0.30(4)	
Ge2	0.0677(2)	3/4	1/4	0.05(4)	
O1	−0.1431(2)	0.0820(2)	0.0135(2)	0.32(4)	
O2	0.0173(1)	0.20213(3)	−0.1290(2)	0.45(4)	
O3	−0.0281(1)	−0.2102(3)	−0.1238(3)	0.64(4)	
O4	−0.1421(2)	0.0438(3)	−0.2873(2)	0.33(4)	
O5	−0.2401(2)	−0.2226(3)	−0.1293(2)	0.86(4)	

cell dimensions. Longer runs for structure refinement were made at 503 K and at room temperature. The phase transition was crossed twice and appeared to be reversible. Subsequently, 45 min runs were performed at 4 °C intervals in the temperature range 433–453 K (six points) and at 2 °C intervals in the range 453–483 K about T_C. These data were used for crystal structure refinements in the vicinity of the transitions.

For $KTaOGeO_4$, long runs for accurate structure refinement were performed at 753 K (HT modification) and at room temperature.

Table 1. (Continued)

High-temperature modification of TlSbOGeO$_4$ at 423 K					
Time of flight data range, 31–121 ms			1880 reflections, 37 structural parameters		
$R_p = 3.67$, $R_w = 4.05$, $(N - P + C) = 4489$			$\chi^2 = 2.02$ for 4541 observations		
$a = 13.372\,69(4)$, $b = 6.677\,87(2)$, $c = 10.768\,44(3)$ Å			space group, *Pnan*		
Atom	x/a	y/b	z/c	ITF	Occupation
Tl1	−0.1403(5)	0.0334(8)	0.3984(8)	2.22(5)	0.408(8)
Tl2	−0.1424(3)	0.0485(5)	0.3410(6)	2.22(5)	0.592(8)
Sb1	0.1302(3)	1/4	1/4	0.76(6)	
Sb2	0	0	0	0.58(5)	
Ge1	1/4	0.0683(3)	0	0.70(4)	
Ge2	0.0681(2)	3/4	1/4	0.68(4)	
O1	−0.1432(2)	0.0825(3)	0.0144(2)	1.06(4)	
O2	0.0170(2)	0.2010(4)	−0.1306(3)	1.15(5)	
O3	−0.0283(2)	−0.2090(4)	−0.1226(3)	1.12(4)	
O4	−0.1415(2)	0.0423(4)	−0.2869(2)	0.98(4)	
O5	−0.2385(2)	−0.2224(4)	−0.1287(3)	1.47(5)	

3. Crystal structure refinements

It was assumed, on the basis of measurements of the physical properties of a single-crystal of TlSbOGeO$_4$ [17], that this crystal is a exception in the group of KTP analogues, and our results confirm this. We therefore begin with the results of the crystal structure refinements of the more typical members of the KTP family, RbSbOGeO$_4$ and KTaOGeO$_4$.

3.1. RbSbOGeO$_4$

As with KTiOPO$_4$ [20], the transition in RbSbOGeO$_4$ is evident from the decrease in the polar axis lattice parameter c with increasing temperature below T_C and its increase above it; the a and b axes increase monotonically with increasing temperature. The absence of a discontinuity in the unit cell volume confirms that the phase transition is continuous second order (figure 1). The T_C of 458 K is close to the temperature of 450 K determined from physical measurements [15]. The atomic coordinates for RbSbOGeO$_4$ at room temperature, determined from x-ray single-crystal diffraction data, were used as a starting point for the refinement on of the HRPD data taken at 300 K: the two methods gave results which were in good agreement.

The crystal structure of the paraelectric modification of the KTP structure type was first determined with good reliability factors R and R_w in a study of TlSbOGeO$_4$ at room temperature [7]. Its atomic coordinates were chosen as the starting point for a refinement of the high-temperature modification of RbSbOGeO$_4$ on the basis of the data collected at 503 K. As in the refinement of the Tl, Sb-compound, the initial model contained a single independent Rb position. The large B_{33} value of the Rb anisotropic temperature factor provided clear evidence for the presence of site splitting as found in TlSbOGeO$_4$. The powder profile refinement (figure 2(*a*)) yielded satisfactory values of the temperature factors for Rb1 and Rb2 with closely equal site occupancies (table 1) and an interatomic distance Rb1–Rb2= 0.709 Å, which is greater than Tl1–Tl2= 0.56 Å [7]. The results for the high-temperature modification of RbSbOGeO$_4$ obtained from x-ray single-crystal [19] and HRPD neutron data agreed well, including the splitting and the small difference in

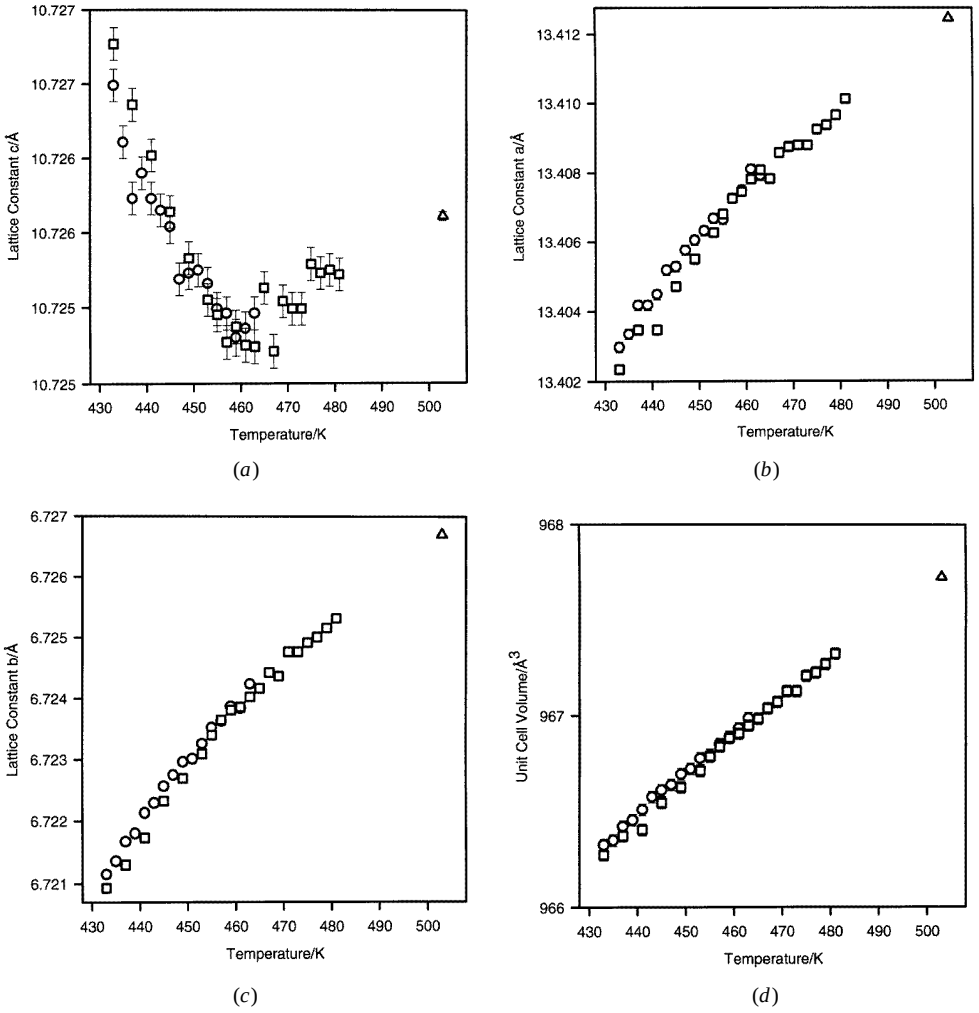

Figure 1. The temperature variation of the orthorhombic unit cell dimensions of $RbSbOGeO_4$: (*a*) *c*, (*b*) *a*, (*c*) *b* and (*d*) the volume.

the site occupancies. The positions of Rb atoms in one-half of unit cell are illustrated in figure 3(*a*).

Data at twenty different temperatures in the interval 433–503 K allowed us to follow the changes in the Rb1 and Rb2 atomic coordinates, which are small and within the range of the standard deviations. This is in contrast to the large displacements found for the K atoms in $KTiOPO_4$ using the same technique [20].

3.2. $KTaOGeO_4$

The polar model refined from the room temperature data agreed well with that found by single-crystal x-ray diffraction methods [8]. The paraelectric crystal structure was refined from the data collected at 753 K, starting from the same model for the paraelectric modification of $TlSbOGeO_4$. As in $RbSbOGeO_4$, the K position in the high-temperature

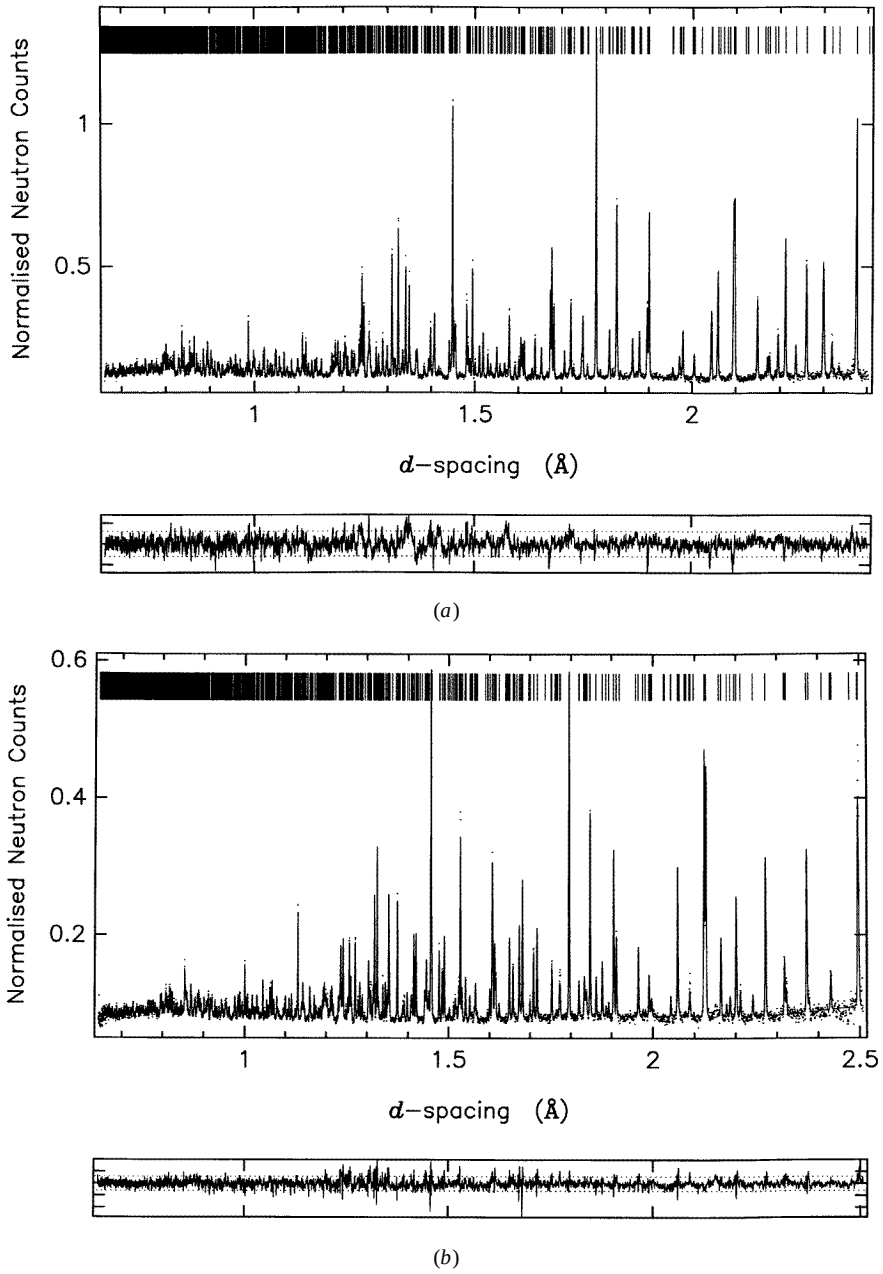

Figure 2. Powder profile refinements of (*a*) $RbSbOGeO_4$ at 503 K and (*b*) $KTaOGeO_4$ at 753 K.

modification was found to be split in the powder profile refinement (figure 2(*b*)). The distance K1–K2= 0.988 Å is more than that found for Tl and Rb (figure 3(*b*)).

The change of Rb and K coordination number is in agreement with previous findings [19, 20]: the coordination decreases from eight or nine in the low-temperature phase to $5+1$ and $4+2$ for Rb1 and Rb2 and to 5 and $4+1$ for K1 and K2 in the high-temperature modification (table 2).

Table 2. Interatomic distances (Å) in high-temperature modifications of KTP-like structures.

		$KTaOGeO_4$	
Ge1,2 tetrahedra		Ta1,2 octahedra	
Ge1–O1(×2)	1.747	Ta1–O3(×2)	1.935
O5(×2)	1.738	O4(×2)	1.992
Ge2–O2(×2)	1.763	O5(×2)	1.975
O4(×2)	1.756	Ta2–O1(×2)	1.997
		O2(×2)	1.962
		O3(×2)	1.967
		K1,2-polyhedra	
K1–O1	2.947	K2–O1	2.692
O2	2.942	O2	2.802
O3	2.881	O3	2.941
O4	2.985	O5	2.737
O5	2.798	O4	3.205
		$RbSbOGeO_4$	
Ge1,2 tetrahedra		Sb1,2 octahedra	
Ge1–O1(×2)	1.748	Sb1–O3(×2)	1.942
O5(×2)	1.727	O4(×2)	2.026
Ge2–O2(×2)	1.756	O5(×2)	1.943
O4(×2)	1.736	Sb2–O1(×2)	2.006
		O2(×2)	1.938
		O3(×2)	1.961
		Rb1,2 polyhedra	
Rb1–O1	2.932	Rb2–O1	2.731
O2	2.910	O2	2.820
O3	2.828	O3	2.864
O4	2.981	O5	2.706
O5	2.776	O4	3.202
O2′	3.277	O4′	3.290

3.3. $TlSbOGeO_4$

Unlike other compounds with the KTP structure, $TlSbOGeO_4$ showed no pronounced anomalies in its cell dimensions at the 272 K transition from the ferroelectric phase to the intermediate structure (figure 4). Further specific heat measurements also showed no anomaly at 272 K, but found one at 286 K, in agreement with the measurements of Stephanovich *et al* [17], who characterized it as a second order phase transition. The change in slope of the unit cell volume versus temperature at 286 K (figure 4(*d*)), confirms that the phase transition is indeed of second order. In [17] it is assumed that the transition is from an antiferroelectric to a paraelectric state.

We carefully checked all our data sets for systematically absent reflections with $h + k = 2n + 1$ in the $hk0$ zone, which would indicate whether the space group was $Pna2_1$ with polar or $Pnan$ with non-polar symmetry. The 260 K data contained a large number of weak or medium-intensity reflections with $h+k = 2n+1$ but no such reflections were present in the data collected at 280 and 423 K, which is consistent with a ferroelectric–paraelectric transition.

The refinement of crystal structure at 260 K was carried out starting from the atomic model determined from the single-crystal x-ray diffraction data collected at 253 K [10]. The results are similar, save for the conclusion that both the Tl sites are split in the polar

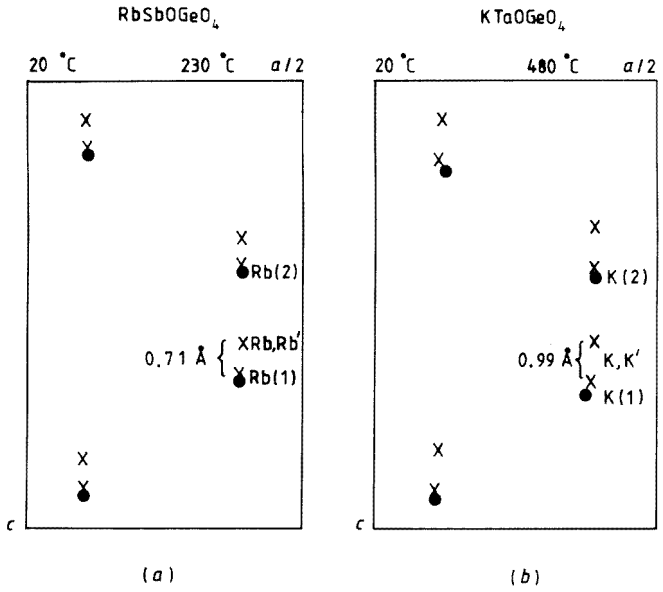

Figure 3. Cation positions at room temperature (black circles) and high temperature (crosses) in (*a*) $RbSbOGeO_4$ (230 °C) and (*b*) $KTaOGeO_4$ (480 °C); the distances in ångströms between the split positions at high temperature are shown.

modification at 260 K (table 1) in comparison with the single split Tl1 site at 253 K found in the x-ray refinement. Amongst the anisotropic temperature parameters determined at 253 K, the B_{33} value of Tl2 was enlarged, which could indicate that the crystal structure was preparing to split this position too. From a consideration of all the x-ray single-crystal and the neutron HRPD data, it is clear that the modification of the crystal structure from low temperature to its transition at $T_C = 272$ K is associated with a maximum polarity at 123 K, which then decreases and disappears at 272 K and may be ascribed (figure 5(*a*)) mainly to the positions occupied by the Tl atoms. At 123 K the Tl1 atoms occupy Tl1 and Tl1′ sites with a small separation of 0.353 Å between them. This splitting may disappear at lower temperatures, since it has not been found at room temperature in other polar KTP modifications having a higher T_C. Atoms in the unsplit Tl2 position have good B_{ij} at 123 K [10]; at 253 K the splitting of the Tl1 position is more pronounced with the distance T1–Tl1′ = 0.527 Å and the B_{33} for Tl2 is three times larger than the other B_{ij} [10]. At 260 K the separation Tl1–Tl1′ increases to 0.716 Å and the Tl2 position is also split.

The results of the x-ray single-crystal [10] and neutron powder refinements at 280 K are in good agreement. Moreover, the split of the Tl position still exists at 423 K (table 1; figure 5(*b*)). The neutron powder profiles taken at 260, 280 and 423 K are illustrated in figure 6(*a*)–(*c*) respectively.

4. Discussion

Pseudosymmetry in KTP-like compounds [21, 22] is the structural basis for the phase transition from a polar, ferroelectric to a nonpolar, paraelectric structure accompanied by the change of space group from $Pna2_1$ to $Pnan$. An important structural feature is the presence of four possible positions for cations within the structure described in space group

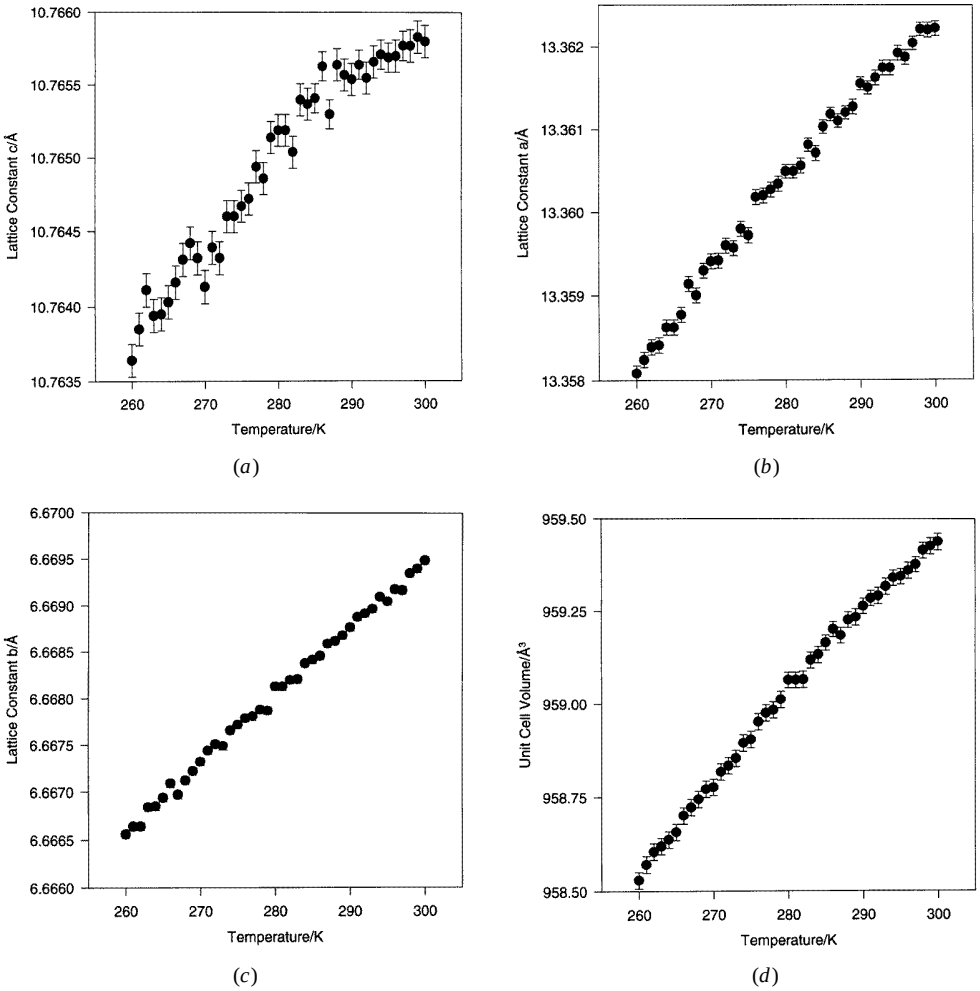

Figure 4. The temperature variation of the orthorhombic unit cell dimensions of $TlSbOGeO_4$: (*a*) *c*, (*b*) *a*, (*c*) *b* and (*d*) the volume.

$Pna2_1$: two of them are occupied and the two pseudosymmetrically related ones are empty. The whole framework of linked octahedra and tetrahedra is described well within the space group $Pnan$ (figure 7). To convert pseudosymmetry to true symmetry, some 'averaging' of the *four* positions of the A cations (two independent positions and two pseudosymmetrically related to them in space group $Pna2_1$) must be made to reduce them to *two* (one independent position in space group $Pnan$).

At room temperature $RbSbOGeO_4$ already possesses high pseudosymmetry which can be characterized by the small linear distortions $D = \Sigma(r_i - r_{av})^2/5$ of its octahedra, $D = 0.0005$ and 0.0007 for Sb1 and Sb2, respectively (in KTP these values are approximately two orders larger, 0.0200 and 0.0140 for Ti1 and Ti2, respectively), so only small displacements of the atoms including Rb are necessary to reach a higher symmetry as the true symmetry. A recalculation of the atomic coordinates in $RbSbOGeO_4$ and $KTaOGeO_4$ from the high-temperature setting in $Pnan$ to the setting in $Pna2_1$, as was performed by Belokoneva *et al*

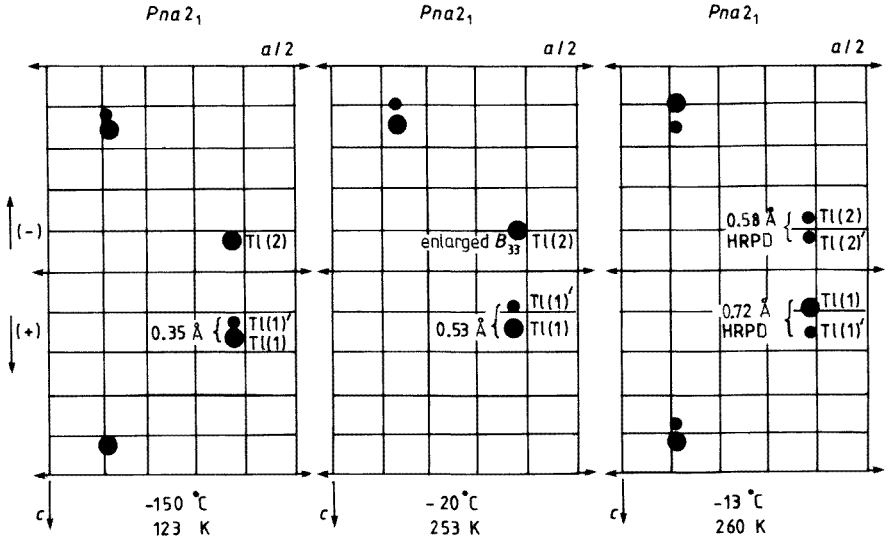

(*a*)

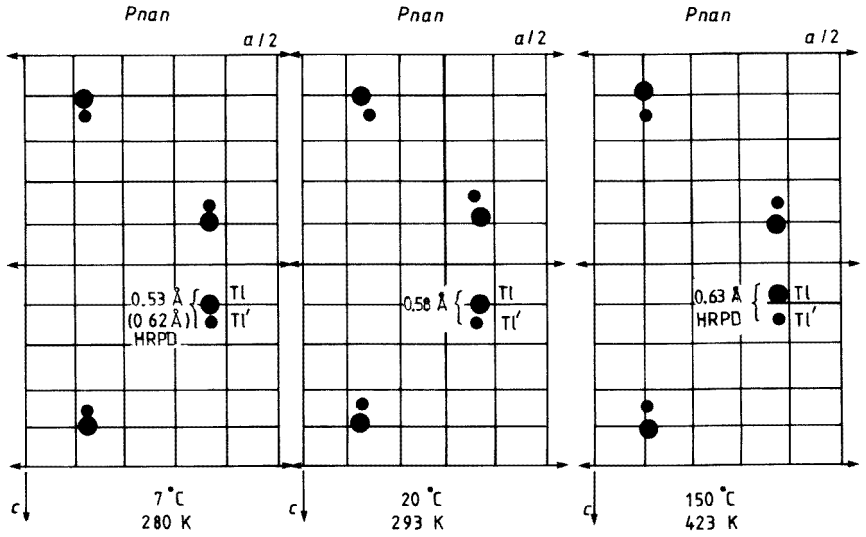

(*b*)

Figure 5. Thallium positions in $TlSbOGeO_4$ at a series of temperatures: (*a*) below $T_C = 272$ K and (*b*) above T_C; the distances in ångströms between split positions are also given.

[10] for $TlSbOGeO_4$, enabled the final displacements of the A and M atoms to be determined in the temperature interval 300–503 K and these are given in table 3. The distortions of the Ta octahedra at room temperature ($D = 0.0014$ and 0.0038 for Ta1 and Ta2, respectively) are almost twice as great as those of the Sb octahedra in $RbSbOGeO_4$. The displacements of the K atoms in $KTaOGeO_4$ between 293 and 753 K are also approximately twice those in $RbSbOGeO_4$ (table 3; figure 3). In all compounds, the A alkali atoms undergo the largest displacements in comparison with other atoms and are principally responsible for the phase transition and appearance and disappearance of P_s.

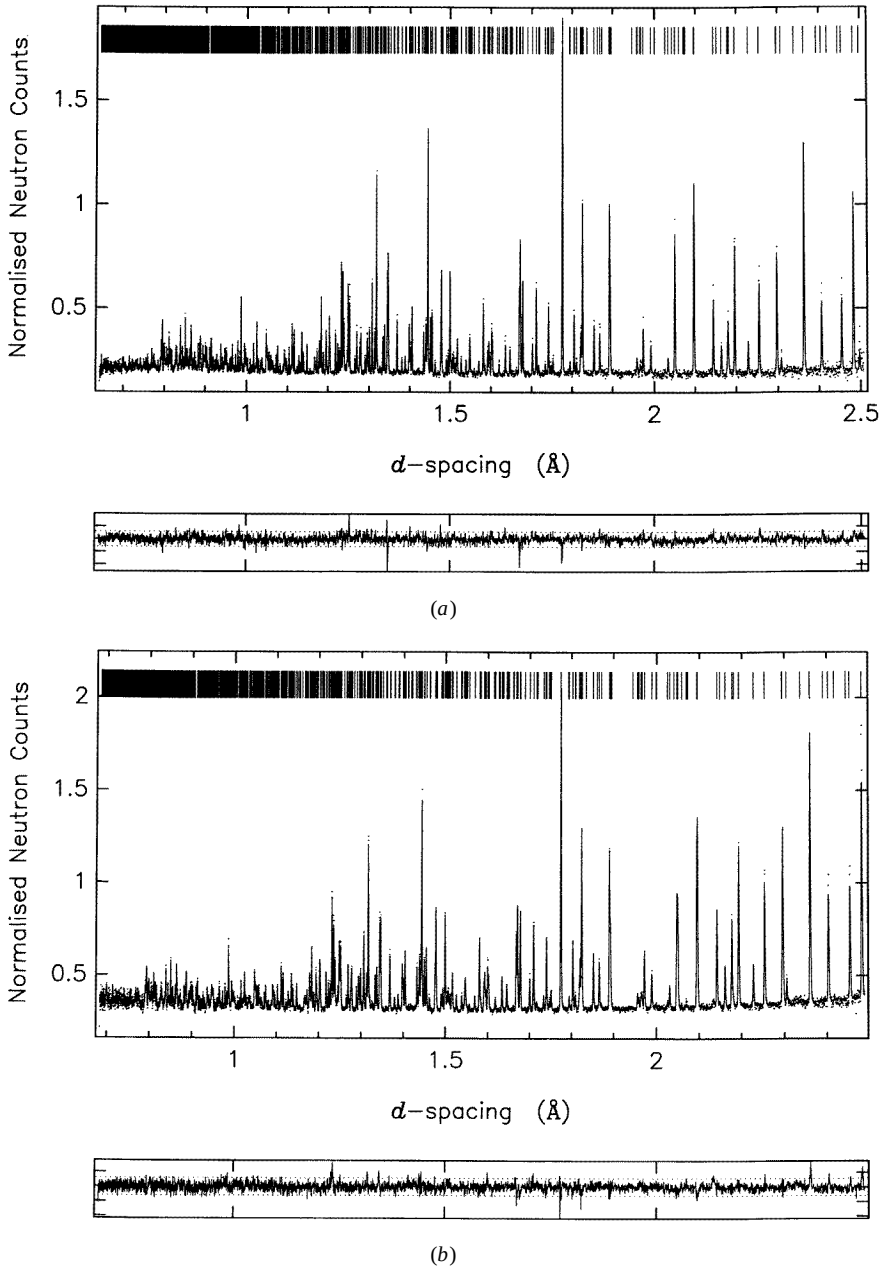

Figure 6. Powder profile refinements of $TlSbOGeO_4$ at (*a*) 260 K, (*b*) 280 K and (*c*) 423 K.

Thus in the high-temperature phase transition of the KTP structure type, small displacements appear for all the atoms followed by doubling of the Rb or K A sites by the twofold axis (figure 3). The phase transition mechanism can be characterized as being both displacive and order–disorder from the structural point of view [23, 10]. The same conclusion was reached by Favard *et al* [19] for other KTP-like silicates and germanates.

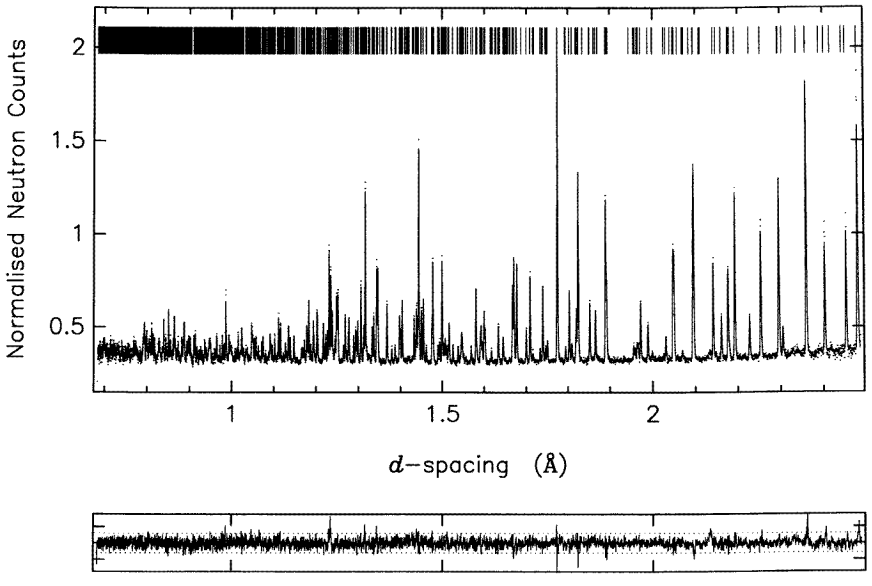

(*c*)

Figure 6. (Continued)

Very small changes in the crystal structure, including the positions of the Tl atoms, are necessary close to the Curie point in $TlSbOGeO_4$ in order to achieve *Pnan* symmetry. This could explain the absence of pronounced anomalies at 272 K in the specific heat curve and in figure 4(*a*) and (*d*). Strong diffuse spots were found on the oscillation photographs made during our single-crystal x-ray study at 280 K [10]. They were not taken into account in determining the crystal structure, which was refined on the basis of the sharp reflection and agreed well with the refinement of the HRPD data collected at the same temperature. No evidence for diffuse scattering appeared in our HRPD pattern at 280 K. Additional single-crystal investigations, especially of diffuse scattering, are necessary to understand the intermediate structural state. At room temperature, oscillation and Weissenberg x-ray single-crystal diffraction photographs show only sharp reflections. The paraelectric state has *Pnan* symmetry and a split Tl position (figure 5(*b*)). On the basis of our results, the phase transition at 286 K is of second order and isostructural without any change of space group (*Pnan*).

It would appear that the occupation of alternative, closely spaced (split) sites is a common and important feature of all high-temperature modifications of KTP-like compounds. In most structures the occupancies of the split sites are approximately equal, but the greatest inequality in occupancy was found in $AgSbOSiO_4$ [5]. The distance between the split positions in the high-temperature modification of the KTP structure type increases in the series $TlSbOGeO_4$, $RbSbOGeO_4$ and $KTaOGeO_4$ and, as we may expect, will be largest in $KTiOPO_4$. The parallel increase in T_C from 272 to 1207 K is connected with less or more pronounced pseudosymmetry in the crystal structure, determined by the framework and mainly by the cation positions in the holes. Thus, at room temperature the coordination polyhedra of the Rb atoms are closer to those of its high-temperature modification and the difference is more pronounced in $KTaOGeO_4$, where T_C is higher. The more polar is the crystal structure at room temperature, the larger are displacements at the phase transition, the greater is the distance between the split alkali metals sites in the 'final' high-temperature

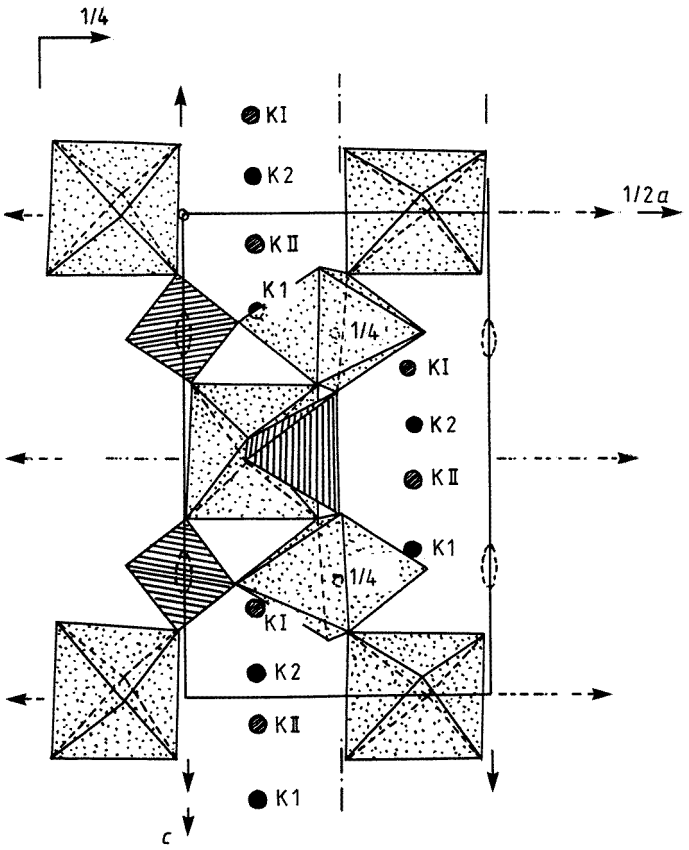

Figure 7. Pseudosymmetry in the KTP structure type. Symmetry elements of the space group $Pna2_1$ and the pseudo-space-group $Pnan$ are shown: K1 and K2 are the real sites; KI and KII are the pseudosymmetrical sites.

modification and the higher T_C. The observed structural changes are therefore in good agreement with the Abrahams–Jamieson–Kurtz (AJK) criteria [24].

We have investigated the role of temperature as the thermodynamic variable in the phase transition. It is interesting to compare our findings with the results of detailed studies by Allan and Nelmes [25] of the influence of high pressure on the $KTiOPO_4$ structure at ambient temperature. The phase transition is found at 5.8 GPa and is described as being isostructural, with the same $Pna2_1$ space group for both modifications. The high-pressure modification is still characterized by distorted Ti octahedra, but there is a drastic loss of optical nonlinearity. The displacements of the potassium atoms at the phase transition have been analysed precisely [25]. Using the pseudosymmetrical approach, it can be concluded that K1 and K2 atoms occupy sites which are intermediate between the occupied and pseudosymmetric sites at ambient temperature and pressure (figures 7 and 8). Recalculating the atomic coordinates gives the positions of K1 (0.3964, −0.2221, −0.3691) and of K2 (0.3862, 0.2013, 0.3671), which are close to being related by a twofold axis parallel to a. We can conclude in accordance with [25] that other regions of the KTP structure may be important for the SHG properties: thus the octahedral distortions are an important, but not a sufficient, condition for the appearance of optical nonlinearity.

Table 3. Atomic coordinates of $RbSbGeO_5$ and the major atomic displacements.

Single-crystal x-ray data 293 K				TOF neutron data 300 K				TOF neutron data recalculated for comparison				Main final displacements Δz of atoms A
Rb1	0.3871	0.7809	0.6637	0.3870	0.7801	0.6630		Rb2	0.3881	0.7844	0.6547	0.0998
Rb2	0.1105	0.7000	0.9229	0.1097	0.6986	0.9156		Rb1	0.1106	0.7000	0.9108	0.1545
Sb1	0.2461	0.2550	0.7540	0.2472	0.2541	0.7406		Sb2	0.25	0.25	0.75	0.0011
Sb2	0.3812	0.5055	0	0.3816	0.5095	0		Sb1	0.3812	0.5	0	0.0161
Ge1	0.4986	0.3182	0.7496	0.4984	0.3171	0.7492		Ge1	0.5	0.3182	0.75	
Ge2	0.1804	0.5085	0.4998	0.1802	0.5085	0.4931		Ge2	0.1796	0.5	0.5	
O1	0.4852	0.4914	0.8749	0.4823	0.4880	0.8705		O5	0.4872	0.5276	0.8777	
O2	0.9928	0.9596	0.1189	0.9937	0.9600	0.1145		O5′	0.9872	0.0276	0.1223	
O3	0.3880	0.1733	0.7399	0.3908	0.1783	0.7328		O1	0.3935	0.1711	0.7320	
O4	0.8984	0.6686	0.2759	0.8980	0.6612	0.2617		O1′	0.8935	0.6711	0.2680	
O5	0.1081	0.2972	0.4615	0.1102	0.3001	0.4491		O4	0.1080	0.2940	0.4613	
O6	0.6070	0.7865	0.5345	0.6057	0.7893	0.5238		O4′	0.6080	0.7940	0.5387	
O7	0.2656	0.5548	0.3838	0.2683	0.5596	0.3742		O2	0.2640	0.5499	0.3788	
O8	0.7643	0.0422	0.6240	0.7612	0.0392	0.6169		O2′	0.7640	0.0499	0.6212	
O9	0.2272	0.9654	0.3784	0.2213	0.9614	0.3648		O3	0.2207	0.9553	0.3745	
O10	0.7182	0.4550	0.6304	0.7203	0.4515	0.6183		O3′	0.7207	0.4 553	0.6255	

$KTaGeO_5$

293 K				293 K				753 K				
K1	0.3743	0.7744	0.6985	0.3748	0.7783	0.6946		K2	0.3846	0.7854	0.6725	0.254
K2	0.1098	0.7074	0.9360	0.1098	0.7014	0.9316		K1	0.1109	0.6924	0.9162	0.184
Ta1	0.2442	0.2601	0.7534	0.2438	0.2612	0.7526		Ta2	0.25	0.25	0.75	0.040
Ta2	0.3840	0.5045	0	0.3838	0.5043	0		Ta1	0.3830	0.50	0	0.016
Ge1	0.4957	0.3222	0.7478	0.4961	0.3224	0.7480		Ge1	0.50	0.3208	0.75	
Ge2	0.1822	0.5047	0.4971	0.1820	0.5041	0.4988		Ge2	0.1810	0.5	0.5	
O1	0.4888	0.4934	0.8667	0.4837	0.4976	0.8644		O5	0.4892	0.5253	0.8767	
O2	0.9944	0.9660	0.1125	0.9960	0.9599	0.1139		O5′	0.9892	0.0253	0.1233	
O3	0.3888	0.1831	0.7324	0.3895	0.1753	0.7332		O1	0.3930	0.1759	0.7308	
O4	0.8987	0.6678	0.2699	0.8980	0.6739	0.2718		O1′	0.8930	0.6759	0.2692	
O5	0.1078	0.3044	0.4610	0.1102	0.2979	0.4603		O4	0.1075	0.2911	0.4641	
O6	0.6073	0.7851	0.5277	0.6065	0.7867	0.5279		O4′	0.6075	0.7911	0.5359	
O7	0.2652	0.5442	0.3739	0.2657	0.5438	0.3770		O2	0.2607	0.5419	0.3752	
O8	0.7565	0.0382	0.6209	0.7577	0.0371	0.6240		O2′	0.7607	0.0419	0.6248	
O9	0.2225	0.9577	0.3742	0.2194	0.9587	0.3724		O3	0.2164	0.9456	0.3771	
O10	0.7114	0.4408	0.6218	0.7135	0.4394	0.6217		O3′	0.7164	0.4456	0.6229	

It has been persuasively demonstrated in a series of publications that the electronic structure of the element in the M octahedral positions determines subtle differences in the crystal structure, including the symmetrization of the octahedra by substitution of Ti by Sn [26], by V^{4+} [27] or by Sb in our case, together with the loss of SHG. The optical nonlinearity appears when the M octahedra contain elements with unfilled 3d orbitals in their theoretical valence state such as Ti or its 4d analogue Nb. Such elements give rise to distorted octahedra, for example, if we substitute Ta by Nb in $KTaOGeO_4$ the intensity of the SHG signal increases almost to that from KTP itself [28]. A quantum chemical description of optical nonlinearity as band gap, mixing of orbitals in the ground state and charge transfer excited state has already been given [1, 26, 27]. The important role of cations in this mechanism has also been mentioned [27, 29] after studies of the effect of substitution chemistry (K by Na or Ag) and its influence on the 'titanyl' bridge oxygens in the chains of Ti octahedra.

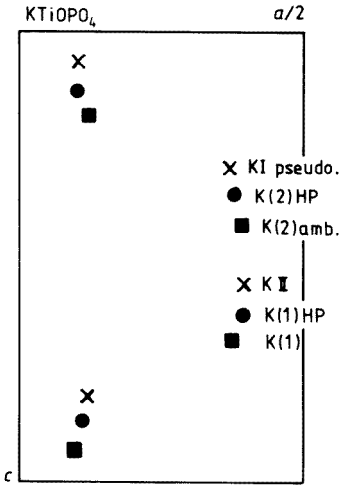

Figure 8. K positions in $KTiOPO_4$ at ambient temperature and pressure (black squares), and at high-pressure (black circles) and the pseudosymmetrical positions (crosses).

The determination of new high-temperature and high-pressure crystal structures gives significant confirmation of the important role played by the A cations in the nonlinear optical properties. The alternating occurrence of short and long bonds in the Ti–O_{bridge} of the octahedron chain is well known. An analysis of the bond lengths in the K–O_{bridge} of $KTiOPO_4$ in ambient conditions also shows a regular, alternating occurrence of long and short bonds: K1–O9 = 2.996 Å, K1–O10 = 2.722 Å; K2–O9 Å = 2.765 Å and K2–O10 = 3.057 Å in symmetrical agreement with Ti2–O9 = 1.733 Å, Ti2–O10 = 2.092 Å, Ti1–O9 = 1.981 Å and Ti1–O10 = 1.716 Å (figure 9(*a*)). The high-pressure modification of KTP at 8.2 kbar (figure 9(*b*)) does not have this short–long K–O bond alternation: K2–O9 = 2.919 Å and K2–O10 = 2.860 Å are both long bonds, whereas K1–O9 = 2.883 Å and L1–O10 = 2.511 Å are both short bonds. We conclude that the geometry found in KTP in ambient conditions, with its alternating distribution of Ti–O and K–O bond lengths (figure 9(*a*)) looks favourable for 'pumping' or anharmonic oscillations of charge (electrons) [27, 30].

The unequal contribution of the short and long Ti–O bonds to the total second-order dielectric susceptibility may be important in Levine's bond charge model [31]. The role of A cations must also be taken into account, because the important bond charges between Ti1–O10 and Ti2–O9 will be determined by the participation of O9 and O10 in bonds with the cations in the cavities. Thus if shorter bond lengths and lower coordination are produced if K is substituted by Ag with its larger electronegativity or simply by the displacement of K atoms under pressure, the part of the bridge oxygen electron density which previously belonged to the Ti–O bond is reduced together with the bond charge and the subtle mechanism of SHG is unbalanced. The effect of the participation of bridge oxygens in different bonds and their role in SHG has been demonstrated in $(NH_4)H(TiOPO_4)$ [32], where the protonation of every other bridge oxygen atom in the Ti–O chain leads to its participation in the O–H bond and consequently to a drastic change in the corresponding Ti–O bond from short to long (figure 9(*c*)), accompanied by a loss of nonlinearity in comparison to $(NH_4)_2(TiOPO_4)_2$.

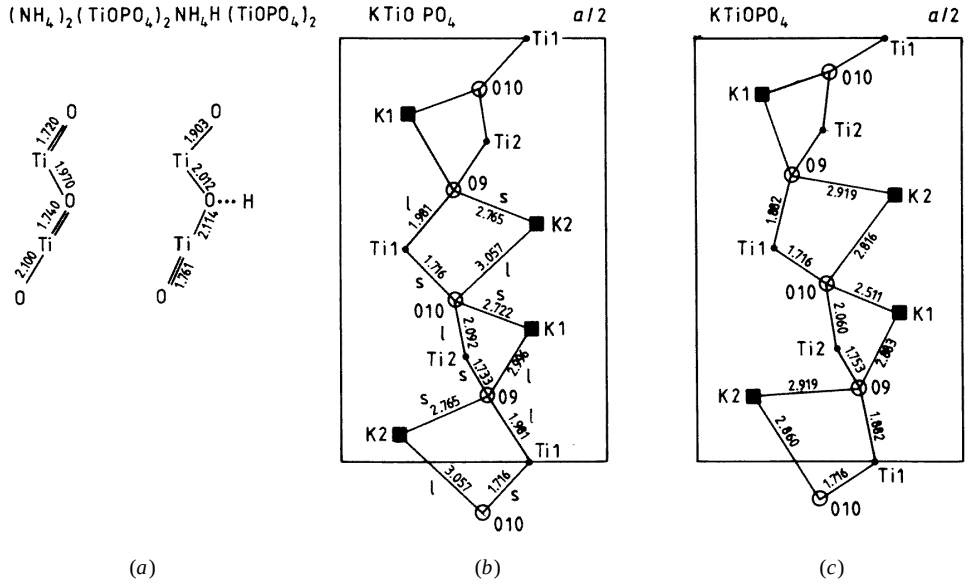

Figure 9. Interatomic distances in the Ti–O and K–O chain of the KTiOPO$_4$ structure (*a*) at ambient temperature and pressure and (*b*) at high pressure; (*c*) the Ti–O chain in $(NH_4)_2(TiOPO_4)_2$ and $NH_4H(TiOPO_4)_2$ [32].

A number of band structure calculations have been carried out [30, 33, 34], but the results are dependent on the dimensions of the cluster [34]. From our results it appears that the A cations should also be taken into account in the calculations, even if this introduces additional difficulties.

5. Conclusion

The temperature-induced ferroelectric–paraelectric phase transition in the KTP structure type, accompanied by a change of space group from $Pna2_1$ to $Pnan$, is determined mainly by the behaviour of the A cations. They have been shown to have the largest displacements amongst all the atoms in the structure and to have split sites in the high-temperature modification. The transition is therefore continuous second order and both displacive and order–disorder in nature, in contrast to the pure displacive phase transition produced by high pressure at ambient temperature. The regularity in the increasing values of T_C found in a series of KTP-like compounds is in agreement with AJK criteria.

Several conditions must be satisfied to produce a second-order term in optical susceptibility and hence nonlinear optical properties in the KTP structure type. The M octahedra must by occupied by transition elements with unfilled 3d or 4d orbitals in their theoretical valence state such as Ti or Nb (but not Sn or Sb). Amongst germanates with weak SHG, substitution of Sb by Nb enhances the signal significantly. In such cases, the distortion of the M octahedra stabilizes a distorted ground state [26]. The redistribution of A cations in the structural holes formed by the framework must be polar, and the cations must not suppress the electronic state of the titanyl bridge oxygens in the chain of octahedra, which is favourable for the existence of a charge transfer excited state delocalized along the TiO_6 chains. Thus both the electronegativities of A cations and their positions in the

cavities are important. The alternating short and long interatomic distances in crystals with good SHG is typical not only for the M–O_{bridge}, but also for the A–O_{bridge}, being very regular in the KTP structure.

Further evidence for the reoccupation of orbitals in the charge transfer excited state may be found from accurate determinations of the electron density by x-ray diffraction from a single crystal illuminated by a laser beam, as reported by Pressprich *et al* [35].

Acknowledgments

The authors wish to thank J B Forsyth for his help in the production of this paper. We are grateful to J A Kaduk, D R Allan and R J Nelmes for letting us know the results of their phase transition investigations of KTP before publication. ELB is indebted to the Royal Society of London for financial support which has enabled her to participate in the ISIS experiments as part of the joint project P737. The samples were prepared as part of INTAS projects 1010-CT-0061 which have contributed greatly to the success of this research.

References

[1] Stucky G D, Phillips M L F and Gier T E 1989 *Chem. Mater.* **1** 492
[2] Belokoneva E L, Mill' B V and Butashin A V 1991 *Izv. Akad. Nauk SSSR, Neorg. Mater.* **27** 1708
[3] Crosnier M-P, Guyomard D, Verbaere A and Piffard Y 1990 *Eur. J. Solid State Inorg. Chem.* **27** 845
[4] Pagnoux C, Guyomard D, Verbaere A, Piffard Y and Tournoux M 1991 *C. R. Acad. Sci. Paris* **312** 611
[5] Mill' B V, Butashin A V and Stephanovich S Yu 1993 *Russ. J. Inorg. Chem.* **38** 947
[6] Mill' B V, Butashin A V and Stephanovich S Yu 1993 *Russ. J. Inorg. Chem.* **38** 1096
[7] Belokoneva E L and Mill' B V 1992 *Russ. J. Inorg. Chem.* **37** 252
[8] Belokoneva E L and Mill' B V 1992 *Russ. J. Inorg. Chem.* **37** 998
[9] Pagnoux C, Favard J-F, Verbaerer A, Piffard Y and Tournoux M 1992 *C. R. Acad. Sci., Paris* **314** 151
[10] Belokoneva E L, Dolgushin F M, Antipin M Yu, Mill' B V and Struchkov Yu T 1993 *Russ. J. Inorg. Chem.* **38** 584
[11] Favard J F, Verbaere A, Piffard Y and Tournoux M 1992 *C. R. Acad. Sci., Paris* **315** 305
[12] Belokoneva E L and Mill' B V 1994 *Russ. J. Inorg. Chem.* **39** 341
[13] Belokoneva E L and Mill' B V 1994 *Russ. J. Inorg. Chem.* **39** 349
[14] Belokoneva E L and Mill' B V 1996 *Russ. J. Inorg. Chem.* **41** 739
[15] Mill' B V, Butashin A V and Stephanovich S Yu 1991 *Kristallographiya* **36** 1481
[16] Simon A, Ravez J, Favard J-F, Verbaere A and Piffard Y 1993 *C. R. Acad. Sci., Paris* **317** 179
[17] Stephanovich S Yu, Mill' B V and Butashin A V 1993 *Kristallographiya* **38** 600
[18] Harrison W T A, Gier T E, Stucky G D and Schulz A J 1990 *J. Chem. Soc. Chem. Commun.* 540
[19] Favard J-F, Verbaire A, Piffard Y and Tournoux M 1994 *Eur. J. Solid State Inorg. Chem.* **31** 995–1008
[20] Kaduk J A, Faber J, Pei S and Jarman R H 1994 *ACA Meeting (Atlanta, 1994) Coll. Abstr.* PIN27, p 141
Kaduk J A, Faber J, Pei S and Jarman R H A 1995 private communication
[21] Belokoneva E L, Yakubovich O V, Tsirel'son V G and Urusov V S 1990 *Izv. Akad. Nauk SSSR, Neorg. Mater.* **26** 595
[22] Thomas P A, Glazer A M and Watts B E 1990 *Acta Crystallogr.* B **46** 333
[23] Belokoneva E L, Knight K S, David W I F and Mill' B V 1995 *ECM16 (Lund, 1995) Coll. Abstr.* P16–25 p 116
[24] Abrahams S 1994 *Acta Crystallogr.* A **50** 658
[25] Allan D R and Nelmes R J 1996 *J. Phys.: Condens. Matter* **3** 2337
[26] Phillips M L F, Harrison W T A and Stucky G D 1990 *Inorg. Chem.* **29** 3245
[27] Phillips M L F, Harrison W T A, Gier T E, Stuky G D, Kulkarny G V and Burdett J K 1990 *Inorg. Chem.* **29** 2158
[28] Butashin A V, Mill B V, Mosunov A V and Stefanovich S Yu 1994 *Russ. J. Inorg. Chem.* **39** 1367
[29] Phillips M L F, Harrison W T A, Stucky G D, McCarron E M, Calabrese I C and Gier T E 1992 *Chem. Mater.* **4** 222
[30] Munowitz M, Jarman R H and Harrison J F 1992 *J. Phys. Chem.* **9** 124
[31] Tsirelson V G and Ozerov R P 1996 *Electron Density and Bonding in Crystals* (Bristol: Institute of Physics)

[32] Eddy M M, Gier T E, Keder N L, Stucky G D, Cox D E, Bierlein J D and Jones G 1988 *Inorg. Chem.* **27** 1856
[33] Munowitz M, Jarman R H and Harrison J F 1992 *Chem. Mater.* **4** 1296
[34] Munowitz M, Jarman R H and Harrison J F 1993 *Chem. Mater.* **5** 661
[35] Pressprich M R, White M A and Coppens P 1994 *Extended Abstr., 11th Sagamore Conf. (Brest, 1994)* vol O4–3, p 166